Electroinduced and Spontaneous Metal−Halide Bond Dissociation in [Co(η^5-C_5H_5)(η^3-2-MeC_3H_4)I]

Maria Gabriela Teixeira,[†] Francesco Paolucci,[‡] Massimo Marcaccio,[‡] Teresa Aviles,[†] Carmen Paradisi,[‡] Flavio Maran,[§] and Sergio Roffia*[,‡]

Departamento de Quimica, Universidade Nova de Lisboa, Monte da Caparica, Lisboa, Portugal, Dipartimento di Chimica, Università di Bologna, Via Selmi 2, 40126 Bologna, Italy, and Dipartimento di Chimica Fisica, Università di Padova, Via Loredan 2, 35131 Padova, Italy

Received July 28, 1997

The electrochemical behavior of the species [Co(η^5-C_5H_5)(η^3-2-MeC_3H_4)I] and [Co(η^5-C_5H_5)(η^3-2-MeC_3H_4)(ACN)]$^+$ in ACN solutions, at 25 °C, is described. The kinetic analysis of the cyclic voltammetry curves indicates that the introduction of one electron in the former complex is concerted with the dissociation of the Co−I bond. The ensuing radical undergoes fast solvation to yield the solvato complex [Co(η^5-C_5H_5)(η^3-2-MeC_3H_4)(ACN)]$^\bullet$, which then acts as an efficient electron donor toward the starting material with the formation of [Co(η^5-C_5H_5)(η^3-2-MeC_3H_4)(ACN)]$^+$; finally, the cation is electroreduced at the working potentials to conclude an overall autocatalytic sequence. The solvato complex [Co(η^5-C_5H_5)(η^3-2-MeC_3H_4)(ACN)]$^\bullet$, formed as a product of the above reduction process, can be reversibly reduced to the corresponding anion at more negative potentials. Confirmation of the above mechanism and of the fact that the solvato complex can act as a solution electron donor toward the starting material was obtained by studying the electrochemical behavior of the solvato complex itself and through calculations aimed to better define the dissociative electron-transfer process to [Co(η^5-C_5H_5)(η^3-2-MeC_3H_4)I]. The dissociation of the metal−halide bond in the neutral complex [Co(η^5-C_5H_5)(η^3-2-MeC_3H_4)I], with the formation of [Co(η^5-C_5H_5)(η^3-2-MeC_3H_4)(ACN)]$^+$, was also found to occur spontaneously, in the bulk, through the observation of a progressive change of the cyclic voltammetric pattern. Support for the occurrence of the reaction between the starting complex and the solvent was confirmed by conductivity and spectroscopic measurements, which allowed the rate constant for the homogeneous solvolysis to be determined.

Introduction

Studies of nucleophilic additions to organotransition metal complexes have led to an increasing interest in the preparation of these species.[1−3] In particular, efforts have been made to synthesize and characterize transition metal complexes able to perform the photo- and/or electrocatalytic activation of carbon dioxide and other small molecules.[4] In this light, many cobalt complexes containing either porphyrinic or non-porphyrinic macrocyclic ligands as well as other ligands, such as diimines and phosphines, with interesting catalytic properties have been synthesized in the past two decades.[1] Transition metal complex mediated cyclization reactions have received much attention in organic synthesis. In particular, η^5-cyclopentadienylCo(I) complexes have been intensively studied and developed into a versatile synthetic method.[2,3] η^5-Cyclopentadienyl Co(III) complexes, also bonded to styrenevinylbenzene copolymers, have been used as hydrogenation and Fischer−Tropsch catalysts.[3] η^5-CyclopentadienylCo complexes often have interesting chemical and physical properties.[3] In particular, they undergo facile electron-transfer reactions accompanied by structural and spectral changes.[5] In light of their possible application in catalytic and electrocatalytic cycles, fundamental information concerning the bonding nature, stereochemistry, reactivity, and electronic structure of such organotransition metal complexes is needed. In particular, as far as the electrochemical properties are concerned, since a drastic influence on the reactivity of these species derives from the charge localization within the

* To whom correspondence should be addressed. Fax: +39-51-259456. E-mail: roffia@ciam.unibo.it.
[†] Universidade Nova de Lisboa.
[‡] Università di Bologna.
[§] Università di Padova.

(1) Ojima, I.; Tzamarioudaki, M.; Li, Z.; Donovan, R. J. *Chem. Rev.* **1996**, *96*, 635 and references therein.

(2) (a) Rybinskaya, M. I. *J. Organomet. Chem.* **1990**, *383*, 113. (b) Krivykh, V. V.; Gusev, O. V.; Rybinskaya, M. I. *J. Organomet. Chem.* **1989**, *362*, 351. (c) Masotti, H.; Wallet, J. C.; Peiffer, G.; Petit, F.; Mortreux, A.; Buono, G. *J. Organomet. Chem.* **1986**, *308*, 241.

(3) (a) King, J. A., Jr.; Vollhardt, P. C. *J. Organomet. Chem.* **1989**, *369*, 245. (b) Ito, Y.; Inouye, M.; Murakami, M.; Shiro, M. *J. Organomet. Chem.* **1989**, *359*, C57. (c) Wakatsuki, Y.; Yoshimura, H.; Yamazaki, H. *J. Organomet. Chem.* **1989**, *366*, 215. (d) Hart, W. P.; Rausch, M. D. *J. Organomet. Chem.* **1988**, *355*, 455. (e) Kuhn, N.; Brüggemann, Winter, M. J.; De Bellis, V. M. *J. Organomet. Chem.* **1987**, *320*, 391. (f) Aviles, T.; Barroso, F.; Royo, P. *J. Organomet. Chem.* **1987**, *326*, 423 and references therein.

(4) (a) Costamagna, J.; Ferraudi, G.; Canales, J.; Vargas *Coord. Chem. Rev.* **1996**, *148*, 248. (b) Collin, J. P.; Sauvage, J. P. *Coord. Chem. Rev.* **1989**, *93*, 24.

(5) Sun, S.; Sweigart, D. A. In *Advances in Organometallic Chemistry*; Stone, F. G. A., West, R., Eds.; Academic Press: San Diego, CA, 1996; Vol. 40 and references therein.

S0276-7333(97)00636-5 CCC: $15.00
Publication on Web 03/03/1998

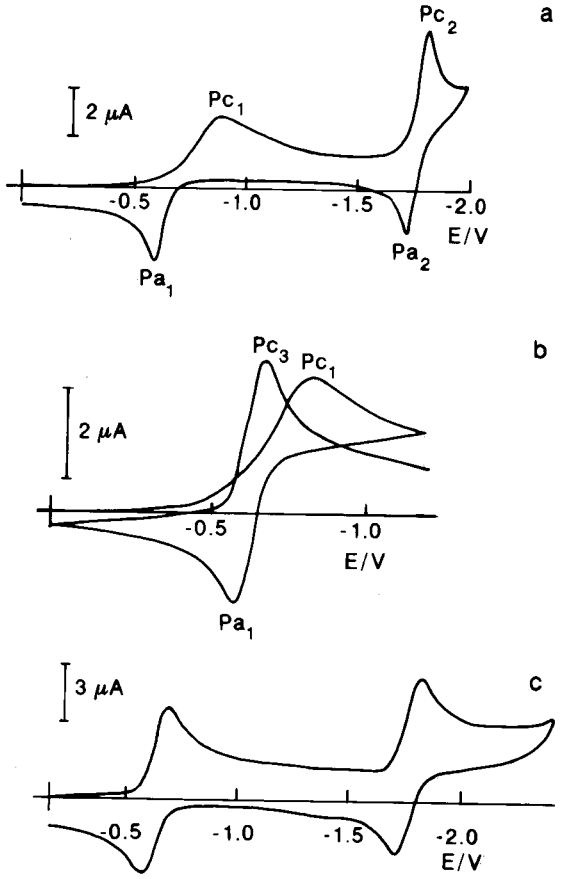

Figure 1. Cyclic voltammetry curves for the reduction of 0.5 mM [Co(η^5-C_5H_5)(η^3-2-MeC_3H_4)I] (curves a and b) and [Co(η^5-C_5H_5)(η^3-2-MeC_3H_4)ACN]BF_4 (curve c) at the Pt electrode in ACN/0.05 M $TEABF_4$, T = 25 °C, v = 0.2 V/s. Both curve a and b were recorded within a few minutes from the dissolution of the complex (see text). Curve b shows two consecutive cyclic voltammetry curves.

reduced molecular electrocatalyst, a detailed description of their electrochemical behavior in terms of both electrode kinetics and redox-site localization is desirable.

In this work, the electrochemical and chemical behavior of the species [Co(η^5-C_5H_5)(η^3-2-MeC_3H_4)I] in acetonitrile (ACN), along with the electrochemical behavior of [Co(η^5-C_5H_5)(η^3-2-MeC_3H_4)(ACN)]BF_4 in the same solvent, is described.

Results and Discussion

Figure 1a shows the cyclic voltammetry (CV) curve for a 0.5 mM ACN solution of [Co(η^5-C_5H_5)(η^3-2-MeC_3H_4)I] in 0.05 M $TEABF_4$ at 25 °C with a scan rate of 0.2 V/s, using a Pt electrode. The same voltammetric pattern was observed with a glassy carbon electrode. The curve was recorded shortly after dissolution of the complex in order to avoid the influence of the chemical reaction between the complex and the solvent (vide infra).

In the potential range explored, two cathodic and two anodic peaks are observed which are denoted as P_{C1}, P_{C2} and P_{A1}, P_{A2}, respectively. The charge associated with each peak corresponds, by comparison with a suitable internal standard (see Experimental Section), to a one-electron charge transfer.

The peak P_{C1} is irreversible with a peak potential E_p = −0.85 V (0.1 V s^{-1}), while peak P_{C2} is reversible with $E_{1/2}$ = −1.78 V. The peak potential E_p of P_{C1} varies linearly with the logarithm of the scan rate by −117 mV per log unit, providing a value of 0.25 for the transfer coefficient α.[6] Its width (i.e., the difference between the value of the potential at half-peak height, $E_{p/2}$, and E_p) is virtually independent of scan rate and equal to 190 mV, leading to the same value for α. To detect a possible dependence of α on electrode potential, analysis of the CV curves at various scan rates was carried out by the logarithmic analysis of the convoluted voltammetric curves of peak P_{C1}.[7,8] However, by also using this procedure, a significant potential dependence of α in the potential range in which measurements could be carried out (0.4 V) was not evident; on the other hand, an average value $\eta = 0.25 \pm 0.05$, coincident with the preceding ones, was obtained. The broadness of the peak and the large slope obtained in the plot of E_p vs log v, indicate that the first reduction of the starting complex is governed by the kinetics of the electron-transfer process.

CV experiments in which a second cathodic scan was initiated immediately at the end of the first cycle, without the renewal of the diffusion layer (Figure 1b), showed that peak P_{A1} represents the anodic partner of a new cathodic peak P_{C3}, which replaces, in the second scan, peak P_{C1}. Thus, peaks P_{C3} and P_{A1} comprise a Nernstian redox couple with $E_{1/2}$ = −0.65 V. Peaks P_{C2}/P_{A2}, corresponding to the redox process with $E_{1/2}$ = −1.78 V, remain unaltered during the second scan. On the basis of the above behavior, peak P_{C3} and its anodic counterpart P_{A1}, therefore, correspond to a reversible charge transfer involving a new electroactive species formed during the reduction of [Co(η^5-C_5H_5)(η^3-2-MeC_3H_4)I]. By considering that the peak P_{A1} is also observed when the first cathodic scan is inverted soon after peak P_{C1}, it follows that the species responsible for peaks P_{C3}/P_{A1} is formed as a result of the first reduction process of [Co(η^5-C_5H_5)(η^3-2-MeC_3H_4)I]. The above results can be summarized in terms of the following mechanism for the reduction of [Co(η^5-C_5H_5)-(η^3-2-MeC_3H_4)I]: the transfer of one electron to the starting complex is accompanied by the formation of a new species, and the kinetics of this irreversible process is governed by the kinetics of the electron-transfer step. The second redox process is the reversible reduction of the new species formed in the first process.

To give a more detailed description of the above reduction mechanism, attention was focused on the identification of the species generated in the first process and on its mechanism of formation. By considering the possibility that at the temperature of the electrochemical experiments the starting complex undergoes thermally induced dissociation of the metal−halide bond accompanied by the coordinaton of a solvent molecule (vide infra), a good candidate for the new species formed in the first process, and responsible for the second peak in the first scan CV curve, is the solvato-complex [Co-

(6) Bard, A. J.; Faulkner, L. R. *Electrochemical Methods, Fundamentals and Applications*; Wiley: New York, 1980; p 223.
(7) (a) Imbeaux, J. C.; Savéant, J.-M. *J. Electroanal. Chem.* **1973**, *44*, 169. (b) Savéant, J.-M.; Tessier, D. *J. Electroanal. Chem.* **1975**, *65*, 57.
(8) Antonello, S.; Musumeci, M.; Wayner, D. D. M.; Maran, F. *J. Am. Chem. Soc.* **1997**, *119*, 9541.

(η^5-C_5H_5)(η^3-2-MeC_3H_4)(ACN)]$^\bullet$. Due to the large excess of ACN molecules with respect to the complex, the solvato complex should be easily formed by fast coordination of an ACN molecule to the intermediate [Co(η^5-C_5H_5)(η^3-2-MeC_3H_4)]$^\bullet$ formed by the reductive cleavage of the Co−I bond of the starting complex. To verify this hypothesis, the solvato complex was synthesized and its cyclic voltammetry (Figure 1c) investigated using the same conditions as in Figure 1a. A comparison of this curve with the voltammetric behavior of [Co(η^5-C_5H_5)-(η^3-2-MeC_3H_4)I] (see Figure 1a) shows that the CV curves are indeed coincident as far as the two redox processes having $E_{1/2}$ at −0.65 and −1.78 V are concerned. Therefore, the two reversible reductions can be described by eqs 1 and 2.

$$[Co(\eta^5\text{-}C_5H_5)(\eta^3\text{-}2\text{-}MeC_3H_4)(ACN)]^+ + e \rightleftarrows [Co(\eta^5\text{-}C_5H_5)(\eta^3\text{-}2\text{-}MeC_3H_4)(ACN)]^\bullet \quad (1)$$

$$[Co(\eta^5\text{-}C_5H_5)(\eta^3\text{-}2\text{-}MeC_3H_4)(ACN)]^\bullet + e \rightleftarrows [Co(\eta^5\text{-}C_5H_5)(\eta^3\text{-}2\text{-}MeC_3H_4)(ACN)]^- \quad (2)$$

Concerning the mechanism of the formation of the intermediate [Co(η^5-C_5H_5)(η^3-2-MeC_3H_4)(ACN)]$^\bullet$, following the reduction of [Co(η^5-C_5H_5)(η^3-2-MeC_3H_4)I], two different reaction pathways must be considered for such a dissociative electron transfer, i.e., the concerted electron-transfer−bond-fragmentation mechanism, in which the intermediate is formed in a single elementary step (eq 3), or the stepwise pathway, in which the intermediate is formed according to two distinct successive steps (eqs 4 and 5) The adiabatic dissociative

$$[Co(\eta^5\text{-}C_5H_5)(\eta^3\text{-}2\text{-}MeC_3H_4)I] + e \rightarrow [Co(\eta^5\text{-}C_5H_5)(\eta^3\text{-}2\text{-}MeC_3H_4)]^\bullet + I^- \quad (3)$$

$$[Co(\eta^5\text{-}C_5H_5)(\eta^3\text{-}2\text{-}MeC_3H_4)I] + e \rightleftarrows [Co(\eta^5\text{-}C_5H_5)(\eta^3\text{-}2\text{-}MeC_3H_4)I]^{\bullet -} \quad (4)$$

$$[Co(\eta^5\text{-}C_5H_5)(\eta^3\text{-}2\text{-}MeC_3H_4)I]^{\bullet -} \rightarrow [Co(\eta^5\text{-}C_5H_5)(\eta^3\text{-}2\text{-}MeC_3H_4)]^\bullet + I^- \quad (5)$$

electron-transfer theory was presented some years ago by Savéant,[9] and the main guidelines to distinguish a concerted electron-transfer mechanism from the stepwise counterpart have been outlined.[8,10−12] Within dissociative electron transfers, detailed mechanistic analysis has been reported for the reduction of organic halides,[10,12] peroxides,[8,11,13] and sulfur compounds.[14,15] A convenient method of distinguishing between a concerted and stepwise mechanism for the electrochemical reactions derives from the analysis of the shape of the voltammetric curve, from its location on the potential scale with respect to the standard potential of the redox process, and from the variation of its location with the scan rate.[10] In particular, the main characteristics of the voltammetric peak in the two cases can be summarized in a rather general way as follows: in the stepwise mechanism, compared to the dissociative ET (electron transfer), the peak is usually sharper (typical $E_{p/2} - E_p$ values are, on average, 50−70 mV instead of 120−170 mV), the E_p is shifted less negatively upon increasing scan rate (typically, on average, by 30−50 mV instead of 100−140 mV upon a 10-fold increase of scan rate), an oxidation peak due to the product of the first electron transfer may be observed at sufficiently high scan rates in the reverse scan, and E_p at low scan rates is not very far from the standard potential of the couple formed by the starting compound and its one-electron reduction product, in contrast to the dissociative electron transfer for which the standard potential relative to the electron-transfer (rate-determining) step (corresponding in our case to eq 3) is much more positive with respect to the reduction potential. This last characteristic for the dissociative electron transfer implies a small value for the transfer coefficient α, distinctly lower (0.2−0.3) than the value at the standard potential, i.e., 0.5. In addition, α is expected to depend on the potential, although such a dependence is small in the case of dissociative electron transfers.[8,10,11,16]

On the basis of the above diagnostic criteria, the reported features of peak P_{C1}, i.e., (i) the broadness of the peak, (ii) the large slope of the E_p vs log v plot, (iii) the fact that the radical anion [Co(η^5-C_5H_5)(η^3-2-MeC_3H_4)]$^{\bullet -}$ is not detected (its oxidation peak is unobserved at scan rates up to 500 V/s), and (iv) the small value of α, strongly suggest that the dissociative reduction of [Co(η^5-C_5H_5)(η^3-2-MeC_3H_4)I] to give the intermediate [Co(η^5-C_5H_5)(η^3-2-MeC_3H_4)]$^\bullet$ occurs according to a concerted rather than a stepwise mechanism. On the basis of the above discussion, the overall mechanism relative to the reduction of [Co(η^5-C_5H_5)(η^3-2-MeC_3H_4)I] can be depicted as shown below where the

$$[Co(\eta^5\text{-}C_5H_5)(\eta^3\text{-}2\text{-}MeC_3H_4)I] + e \rightarrow [Co(\eta^5\text{-}C_5H_5)(\eta^3\text{-}2\text{-}MeC_3H_4)]^\bullet + I^- \quad (3)$$

$$[Co(\eta^5\text{-}C_5H_5)(\eta^3\text{-}2\text{-}MeC_3H_4)]^\bullet + ACN \rightarrow [Co(\eta^5\text{-}C_5H_5)(\eta^3\text{-}2\text{-}MeC_3H_4)(ACN)]^\bullet \quad (6)$$

$$[Co(\eta^5\text{-}C_5H_5)(\eta^3\text{-}2\text{-}MeC_3H_4)(ACN)]^\bullet + e \rightleftarrows [Co(\eta^5\text{-}C_5H_5)(\eta^3\text{-}2\text{-}MeC_3H_4)(ACN)]^- \quad (2)$$

couple of eqs 3, 6, and eq 2 refer to the first and second reduction processes, respectively.

The dissociative nature of the heterogeneous electron transfer undergone by [Co(η^5-C_5H_5)(η^3-2-MeC_3H_4)I] is also sustained by the other considerations. Usually, the detection of a potential dependence of the transfer coefficient α is quite useful in the analysis of heterogeneous dissociative electron transfers, as found with both

(9) Savéant, J.-M. *J. Am. Chem. Soc.* **1987**, *109*, 6788.
(10) Savéant, J.-M. In *Advances in Electron-Transfer Chemistry*; Mariano, P. S., Ed.; JAI press: Greenwich, 1994; Vol. 4, p 53.
(11) Antonello, S.; Maran, F. *J. Am. Chem. Soc.* **1997**, *119*, 12595.
(12) (a) Savéant, J.-M. *Adv. Phys. Org. Chem.* **1990**, *26*, 1. (b) Savéant, J.-M. *Acc. Chem. Res* **1993**, *26*, 455.
(13) (a) Workentin, M. S.; Maran, F.; Wayner, D. D. M. *J. Am. Chem. Soc.* **1995**, *117*, 2120. (b) Donkers, R. L.; Maran, F.; Wayner, D. D. M.; Workentin, M. S. Manuscript in preparation.
(14) Severin, M. G.; Farnia, G.; Vianello, E.; Arévalo, M. C. *J. Electroanal. Chem.* **1988**, *251*, 369.
(15) Andrieux, C. P.; Robert, M.; Saeva, F. D.; Savéant J.-M. *J. Am. Chem. Soc.* **1994**, *116*, 7864.
(16) Andrieux, C. P.; Gallardo, I.; Savéant, J.-M.; Su, K. B. *J. Am. Chem. Soc.* **1986**, *108*, 638.

organic halides[16] and peroxides.[8,11] In the present study, however, the failure to observe a variation of α with the electrode potential was not totally surprising in view of the nature of the experimental system that was under investigation: in fact, a possible variation was most likely hidden by the experimental uncertainty associated with the parallel occurrence of the thermally induced dissociation of the pristine complex and the effect of a following solution electron transfer (vide infra). On the other hand, the overall uncertainty in the potential range that could be explored (ca. 0.4 V) is in agreement with a maximum value for the potential dependence of α of 0.25 V^{-1}, which is quite in line with what is usually observed with dissociative-type systems.[8,11,16] According to this estimate and by remembering that α is 0.5 at the dissociative electron-transfer standard potential,[10] the latter is at least 0.8 V more positive than the actual position of the experimental peak of [Co(η^5-C_5H_5)(η^3-2-MeC_3H_4)I].

To test the reliability of such a piece of information, some further calculations can be carried out; the potential dependence of α is in fact linked to the intrinsic barrier of the electron-transfer process, $\Delta G_0^{\ddagger}$ (i.e., the activation energy at zero driving force), through $\partial\alpha/\partial E = F/8\Delta G_0^{\ddagger}$.[8] Accordingly, a likely estimate of the miminum value of $\Delta G_0^{\ddagger}$ is 11.5 kcal/mol. On the other hand, in the framework of the current dissociative ET theory, $\Delta G_0^{\ddagger}$ is given by (λ + BDE)/4, where λ is the solvent reorganization energy and BDE the bond dissociation energy. For a dissociative electron transfer a good way to calculate the heterogeneous λ is to use the Marcus expression and an effective radius for the substrate;[8] the latter was calculated starting from the radii of cobaltacene (3.7 Å) and decamethylcobaltacene (4.8 Å)[17] as bracketing the radius of our substrate, by using a two-spheres approach[8,10] that stresses the fact that in a dissociative electron transfer much of the solvent reorganization occurs around the incipient leaving group, I^-. This procedure leads to a λ value bracketed between 12.9 and 14.2 kcal/mol. The intrinsic barrier is finally calculated by using the Co−I BDE available from literature results (34.6 kcal/mol),[18] leading to $\Delta G_0^{\ddagger}$ = 12 kcal/mol. Obviously, this estimate is very approximate, but nevertheless, the agreement between the two independent calculations is worth noting.

Besides enforcing the dissociative electron-transfer mechanism, it is also relevant in the present context that the standard potential for the reduction of [Co(η^5-C_5H_5)(η^3-2-MeC_3H_4)I] is much more positive than the position of the peak. Since [Co(η^5-C_5H_5)(η^3-2-MeC_3H_4)(ACN)]$^{\bullet}$ forms in the reaction layer and by taking into account that the $E_{1/2}$ for its formation is −0.65 V, it results that the homogeneous electron transfer shown in eq 7 has a reaction free energy $\Delta G°$ that is at least −0.6 eV. Therefore, the electron-transfer reaction in eq 7 must be taken into account in the overall process occurring during the reduction of [Co(η^5-C_5H_5)(η^3-2-MeC_3H_4)I]. An approximate estimate of the rate constant of reaction 7 can be obtained by using a conventional equation relating the electron-transfer rate

$$[Co(\eta^5\text{-}C_5H_5)(\eta^3\text{-}2\text{-}MeC_3H_4)I] + [Co(\eta^5\text{-}C_5H_5)(\eta^3\text{-}2\text{-}MeC_3H_4)(ACN)]^{\bullet} \rightarrow [Co(\eta^5\text{-}C_5H_5)(\eta^3\text{-}2\text{-}MeC_3H_4)]^{\bullet} + I^- + [Co(\eta^5\text{-}C_5H_5)(\eta^3\text{-}2\text{-}MeC_3H_4)(ACN)]^+ \quad (7)$$

constant to the free energy of activation $\Delta G^{\ddagger}$, the latter being expressed through the Savéant equation for dissociative electron transfers,[9] i.e., $\Delta G^{\ddagger} = \Delta G_0^{\ddagger}(1 + \Delta G°/4\Delta G_0^{\ddagger})^2$. By using 10^{11} M^{-1} s^{-1} for the preexponential factor (adiabatic electron transfer) and $\Delta G_0^{\ddagger}$ = 15.2 kcal/mol (obtained by using the cobaltacene radius and the Marcus expression for the homogeneous λ), the ensuing rate constant is 2×10^4 $M^{-1}s^{-1}$, although larger values can be obtained by increasing the driving force or using different ways to calculate the homogeneous λ[10,13] and smaller values if the process in nonadiabatic.[13] In Figure 2a is reported the simulation that was performed to reproduce the experimental CVs of Figures 1a and 1b. The rate constant of the electron-transfer reaction 7 was set to 3×10^3 M^{-1} s^{-1}, which is the minimum value necessary to observe the complete disappearance of the P_{C1} peak during the second cycle; concerning reaction 6, the simulation of the voltammetric pattern is independent of the value of the corresponding pseudo-first-order rate constant as long as the latter is $>10^4$ s^{-1}, a condition which is more than reasonable for a solvation process. As can be seen in Figure 2a, the inclusion of reaction 7 in the simulation of the electrode process leads to a quite satisfactory reproduction of the experimental pattern depicted in Figure 1b; as a matter of fact, if the simulation is carried out by neglecting the electron-transfer reaction 7, the peak P_{C1} is still detectable during the second scan after the P_{C1} component (Figure 2b). On the other hand, even a small increase of the rate constant of reaction 7 with respect to the 3×10^3 M^{-1} s^{-1} value causes the simulation to deviate significantly from the experimental pattern; in particular, if the value is progressively increased from 3×10^3 M^{-1} s^{-1} to reach the diffusion-limited value, the peak P_{C1} shifts toward more positive potentials and changes in shape until it becomes coincident with P_{C3}.

By considering that [Co(η^5-C_5H_5)(η^3-2-MeC_3H_4)(ACN)]$^+$ formed by reaction 7 is reducible according to eq 1 at the potentials at which P_{C1} develops, the following autocatalytic dissociative electron-transfer mechanism can be proposed for the first reduction process of [Co(η^5-C_5H_5)(η^3-2-MeC_3H_4)I]:

$$[Co(\eta^5\text{-}C_5H_5)(\eta^3\text{-}2\text{-}MeC_3H_4)I] + e \rightarrow [Co(\eta^5\text{-}C_5H_5)(\eta^3\text{-}2\text{-}MeC_3H_4)]^{\bullet} + I^- \quad (3)$$

$$[Co(\eta^5\text{-}C_5H_5)(\eta^3\text{-}2\text{-}MeC_3H_4)]^{\bullet} + ACN \rightarrow [Co(\eta^5\text{-}C_5H_5)(\eta^3\text{-}2\text{-}MeC_3H_4)(ACN)]^{\bullet} \quad (6)$$

$$[Co(\eta^5\text{-}C_5H_5)(\eta^3\text{-}2\text{-}MeC_3H_4)(ACN)]^{\bullet} + [Co(\eta^5\text{-}C_5H_5)(\eta^3\text{-}2\text{-}MeC_3H_4)I] \rightarrow [Co(\eta^5\text{-}C_5H_5)(\eta^3\text{-}2\text{-}MeC_3H_4)(ACN)]^+ + [Co(\eta^5\text{-}C_5H_5)(\eta^3\text{-}2\text{-}MeC_3H_4)]^{\bullet} + I^- \quad (7)$$

(17) Fawcett, W. R.; Foss, C. A., Jr. *J. Electroanal. Chem.* **1989**, *270*, 103.

(18) Toscano, P. J.; Seligson, A. L.; Curran, M. T.; Skrobutt, A. T.; Sonnenberger, D. C. *Inorg. Chem.* **1989**, *28*, 166.

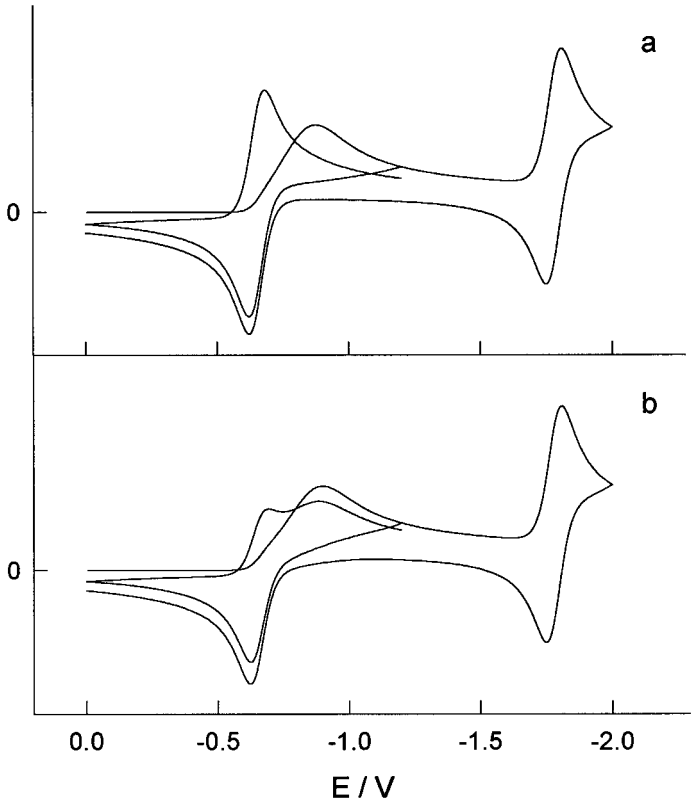

Figure 2. Simulation (DigiSim 2.1) of the experimental voltammetric pattern (cfr. Figure 1a and 1b). The simulations of curves a and b were carried out by using a quadratic activation-driving-force relationship (intrinsic barrier = 11.5 kcal/mol). Whereas curve a shows the effect of the solution electron-transfer reaction 7 (rate constant = 3×10^3 $M^{-1}s^{-1}$), in curve b reaction 7 was not included.

$$[Co(\eta^5\text{-}C_5H_5)(\eta^3\text{-}2\text{-}MeC_3H_4)(ACN)]^+ + e \rightleftarrows [Co(\eta^5\text{-}C_5H_5)(\eta^3\text{-}2\text{-}MeC_3H_4)(ACN)]^{\bullet} \quad (1)$$

The autocatalytic process caused by the succession of reactions 7 and 1 in the above mechanism is, thus, responsible for the disappearance of the peak P_{C1} in the second cathodic sweep. Such a result underlines the importance of the analysis of multisweep voltammetry as a tool in the study of electrode mechanisms.

The CV behavior so far discussed for [Co(η^5-C_5H_5)-(η^3-2-MeC_3H_4)I] refers to freshly made solutions, i.e., those analyzed within ca. 5 min from dissolution of the complex. A progressive variation of the CV curve pattern then becomes apparent. In Figure 3, CV curves recorded under the same conditions used in Figure 1, as a function of time from the dissolution of the compound (time zero), are shown. The shape of the first reduction peak evolves with time, while the remaining part of the curve is invariant. A limiting pattern is reached within 45 min. After that time, two reversible reduction peaks are observed with $E_{1/2}$ values of −0.65 and −1.65 V, respectively. At the intermediate stages, the first reduction peak shows a complex pattern, which suggests the occurrence of two reduction processes, the overall charge exchanged corresponding to a one-electron charge transfer. At lower temperatures (−40 °C), the same evolution of the CV curve to the limiting pattern occurs but on a longer time scale. The coincidence of the $E_{1/2}$'s for the two reduction peaks observed after ≥45 min from the dissolution of the complex with those for the corresponding processes observed under the same conditions for [Co(η^5-C_5H_5)(η^3-2-MeC_3H_4)-(ACN)]$^+$ suggests that the process responsible for the time dependence of the CV curve of [Co(η^5-C_5H_5)(η^3-2-MeC_3H_4)I] is the homogeneous solvolysis of the latter to [Co(η^5-C_5H_5)(η^3-2-MeC_3H_4)(ACN)]$^+$, occurring in the bulk solution according to eq 8

$$[Co(\eta^5\text{-}C_5H_5)(\eta^3\text{-}2\text{-}MeC_3H_4)I] + ACN \rightarrow [Co(\eta^5\text{-}C_5H_5)(\eta^3\text{-}2\text{-}MeC_3H_4)(ACN)]^+ + I^- \quad (8)$$

The CV curves recorded at 10 min ≤ t ≤ 45 min would, therefore, show the cathodic peak deriving from the superposition of two reduction peaks, the first one at less negative potentials due to the reversible reduction of [Co(η^5-C_5H_5)(η^3-2-MeC_3H_4)(ACN)]$^+$ formed in reaction 8 and the second one due to the irreversible dissociative reduction of the complex [Co(η^5-C_5H_5)(η^3-2-MeC_3H_4)I]. The relative contributions of these two peaks would vary with time according to the variation of the concentrations of the two species.

Support for the occurrence of reaction 8 has been obtained by conductivity measurements. Figure 4 shows the variation of the conductivity at 25 °C for a 0.5 mM ACN solution of [Co(η^5-C_5H_5)(η^3-2-MeC_3H_4)I]. The increase of the molar conductivity (Λ) with time, up to a limiting value of 118 S cm^2 mol^{-1}, is attributed to the formation of ionic species according to reaction 8. To obtain information on the extent of reaction, the limiting value, which represents an equilibrium value, has been compared with that expected for the complete dissociation of [Co(η^5-C_5H_5)(η^3-2-MeC_3H_4)(ACN)]I. Since the salts of the cationic species [Co(η^5-C_5H_5)(η^3-2-MeC_3H_4)(ACN)]$^+$ are obtained by removing iodide in

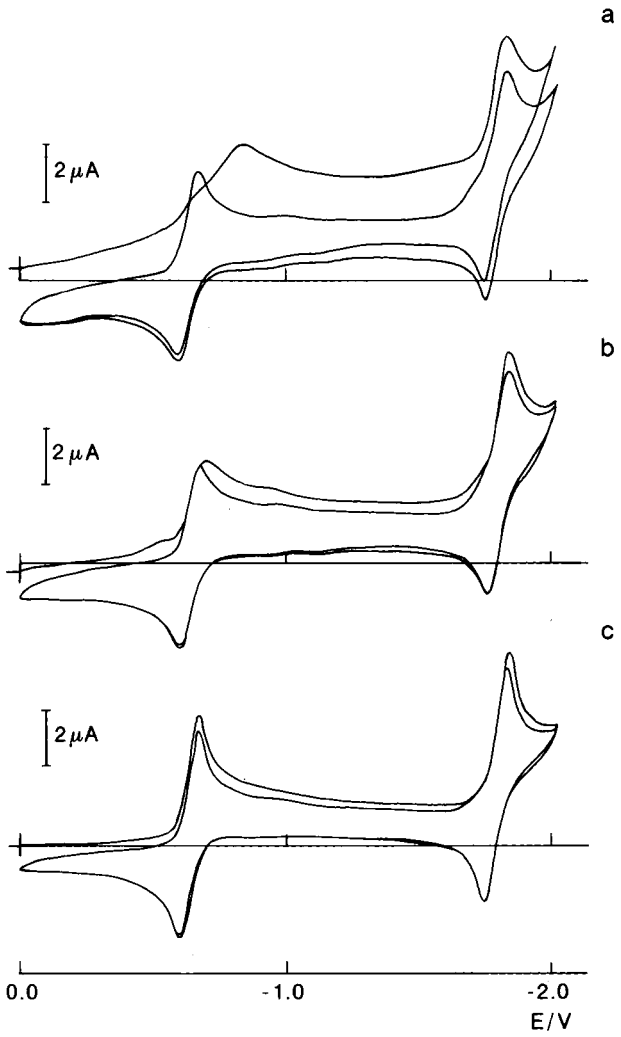

Figure 3. Consecutive cyclic voltammetry curves for a 0.5 mM [Co(η^5-C_5H_5)(η^3-2-MeC_3H_4)I], 0.05 M $TEABF_4$, ACN solution, T = 25 °C, v = 0.2 V/s, working electrode = Pt. Curves recorded after (a) 10, (b) 30, and (c) 45 min of dissolution of the complex (see text).

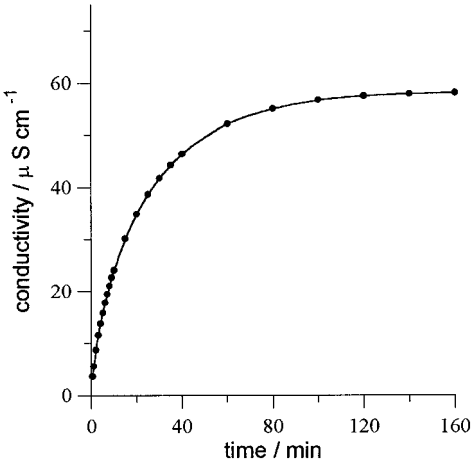

Figure 4. Time evolution of the specific conductivity of a 0.5 mM [Co(η^5-C_5H_5)(η^3-2-MeC_3H_4)I] ACN solution, T = 25.0 °C.

[Co(η^5-C_5H_5)(η^3-2-MeC_3H_4)I] by a silver salt, typically $AgBF_4$, and removing AgI by filtration,[19] a sample of the species [Co(η^5-C_5H_5)(η^3-2-MeC_3H_4)(ACN)]I was not available. Therefore, Λ was obtained for this species by measuring the molar conductivities Λ of ACN solutions of [Co(η^5-C_5H_5)(η^3-2-MeC_3H_4)(ACN)]BF_4, $TEABF_4$, and TEAI under the same conditions used in Figure 4. For the low ion concentrations utilized, the ionic conductivities of the ions, λ_i's, are independent of the nature of the associated ion, i.e., they follow Kohlrausch's law of independent migration.[20] Assuming that in ACN [Co(η^5-C_5H_5)(η^3-2-MeC_3H_4)(ACN)]BF_4, $TEABF_4$, and TEAI are completely dissociated, the following relations hold:

$$\Lambda_{[Co(\eta^5\text{-}C_5H_5)(\eta^3\text{-}2\text{-}MeC_3H_4)(ACN)]I} = \lambda_{[Co(\eta^5\text{-}C_5H_5)(\eta^3\text{-}2\text{-}MeC_3H_4)(ACN)]^+} + \lambda_{I^-} = \lambda_{[Co(\eta^5\text{-}C_5H_5)(\eta^3\text{-}2\text{-}MeC_3H_4)(ACN)]^+} + \lambda_{BF_4^-} - \lambda_{TEA^+} - \lambda_{BF_4^-} + \lambda_{TEA^+} + \lambda_{I^-} = \Lambda_{[Co(\eta^5\text{-}C_5H_5)(\eta^3\text{-}2\text{-}MeC_3H_4)(ACN)]BF_4} - \Lambda_{TEABF_4} + \Lambda_{TEAI}$$

from which, if Λ for the three salts [Co(η^5-C_5H_5)(η^3-2-MeC_3H_4)(ACN)]BF_4, $TEABF_4$, and TEAI is known, the value for $\Lambda_{[Co(\eta^5\text{-}C_5H_5)(\eta^3\text{-}2\text{-}MeC_3H_4)(ACN)]I}$ can be computed. The Λ values for 5.00×10^{-4} M solutions of [Co(η^5-C_5H_5)(η^3-2-MeC_3H_4)(ACN)]BF_4, $TEABF_4$, and TEAI were 144.2, 201.9, and 177.3 S cm^2 mol^{-1}, respectively. Using these values in the above relations, 119.1 S cm^2 mol^{-1} was obtained as the expected Λ value for a completely dissociated 5.00×10^{-4} M [Co(η^5-C_5H_5)(η^3-2-MeC_3H_4)(ACN)]I solution. Comparison of this value with the experimental value (118.2 S cm^2 mol^{-1}) indicates that the dissociation of [Co(η^5-C_5H_5)(η^3-2-MeC_3H_4)I] is practically complete (99.2%) in the conditions reported.

The formation of a 1:1 electrolyte according to eq 8 is also confirmed by the very similar slopes of the ($\Lambda_o - \Lambda$) vs $c^{1/2}$ plots, where Λ_o is the molar conductivity at infinite dilution and Λ that of the solution having molar concentration c, obtained for [Co(η^5-C_5H_5)(η^3-2-MeC_3H_4)I] and for electrolytes with the same anion or anions of similar λ_o respectively.[21] For example, in Figure 5, the plots of ($\Lambda_o - \Lambda$) vs $c^{1/2}$ for [Co(η^5-C_5H_5)(η^3-2-MeC_3H_4)I] and TEAI, a standard 1:1 electrolyte, are shown. The two straight lines fitting the experimental values are practically coincident. In the case of [Co(η^5-C_5H_5)(η^3-2-MeC_3H_4)I], the Λ values used in the plots were always measured at the various initial c's after the equilibrium value had been reached. For all electrolytes, Λ_o has been evaluated as the limiting value of Λ for $c \rightarrow 0$ in the Λ vs $c^{1/2}$ plots.

Finally, the data of Figure 4 were utilized for the determination of the pseudo-first-order rate constant for reaction 8, k_8. The data plotted according to the Guggenheim method[22] as $\ln(\Lambda_{t'} - \Lambda_t)$ vs time, where Λ and $\Lambda_{t'}$ are the molar conductivities at time t and $t' = t$

(19) Aviles, T.; Barroso, F.; Royo, P. *J. Organomet. Chem.* **1982**, *236*, 101.
(20) MacInnes, D. A. *The Principles of Electrochemistry*; Dover Publishing, Inc.: New York, 1961; Chapter 18
(21) (a) Feltham, R. D.; Hayter, R. G. *J. Chem. Soc.* **1964**, 4587. (b) Boggess, R. K.; Zatko, D. A. *J. Chem. Educ.* **1975**, *52*, 649. (c) Weaver, T. R.; Meyer, T. J.; Adeyemi, S. A.; Brown, G. M.; Eckberg, R. P.; Hatfield, W. E.; Johnson, E. C.; Murray, R. W.; Untereker, D. *J. Am. Chem. Soc.* **1975**, *97*, 3039. (d) Rillema, D. P.; Callahan, R. W.; Mack, K. B. *Inorg. Chem.* **1982**, *21*, 2589. (e) Bignozzi, C. A.; Roffia, S.; Chiorboli, C.; Davila, J.; Indelli, M. T.; Scandola, F. *Inorg. Chem.* **1989**, *28*, 4350.
(22) Frost, A. A.; Pearson, R. G. *Kinetics and Mechanism*; Wiley: New York, 1961

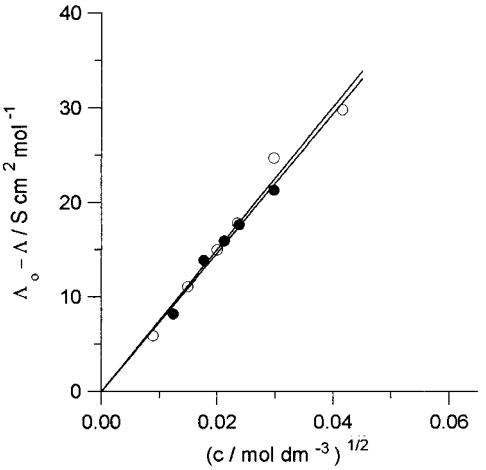

Figure 5. Plots of ($\Lambda_o - \Lambda$) vs $c^{1/2}$ from the conductivity data in ACN at 25.0 °C for [Co(η^5-C_5H_5)(η^3-2-MeC_3H_4)I] (○) and for TEAI (●).

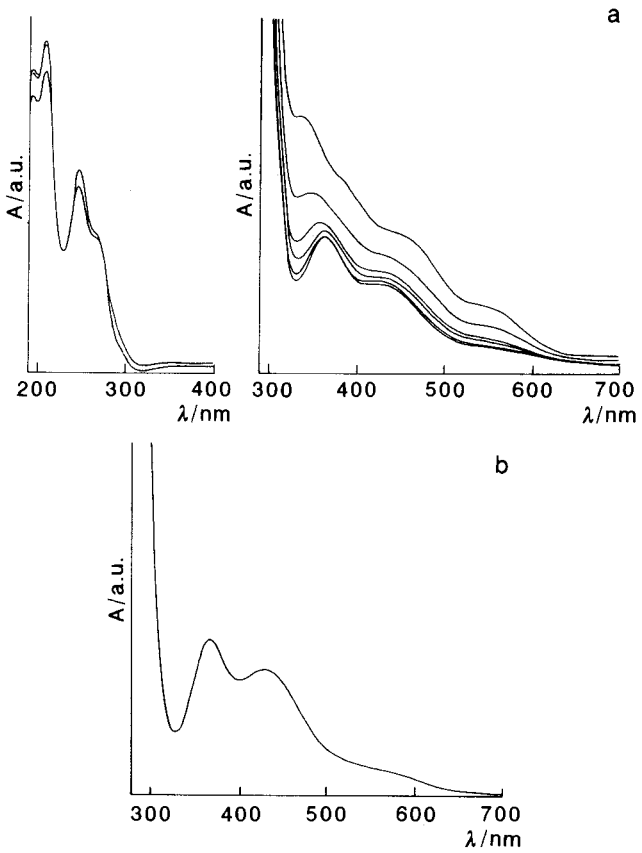

Figure 6. (a) Time evolution of the UV−Vis absorption spectra for a 0.5 mM [Co(η^5-C_5H_5)(η^3-2-MeC_3H_4)I] ACN solution. (b) Visible absorption spectra for a 0.5 mM [Co(η^5-C_5H_5)(η^3-2-MeC_3H_4)ACN]BF_4 ACN solution, T = 25 °C.

+ 20 min, respectively, yielded a linear plot from whose slope the value $k_8 = (5.82 \pm 0.05) \times 10^{-4}$ s^{-1} was obtained.

Besides the variation in the solution conductivity, spectral changes accompany the occurrence of reaction 8, as shown in Figure 6a. The UV−vis spectra for a 0.5 mM solution of [Co(η^5-C_5H_5)(η^3-2-MeC_3H_4)I] in ACN, at 25 °C, were recorded at various times within the first 45 min from the preparation of the solution. After that time, no significant changes in the spectra were observed. The absorption in the visible region decreased with time, while an increase in the UV region was observed, with two isosbestic points at 216 and 275 nm. The final spectrum, recorded at $t \geq 45$ min, coincided with that relative to a solution of pristine [Co(η^5-C_5H_5)(η^3-2-MeC_3H_4)(ACN)]$^+$ under the same conditions, as shown in Figure 6b. Determination of the rate constant k_8 from the spectroscopic data was obtained according to standard procedure.[22] The absorbance values at 367 and 338 nm from the spectra of Figure 6b and the corresponding values for the molar extinction coefficients ϵ_R and ϵ_P at those wavelengths for [Co(η^5-C_5H_5)(η^3-2-MeC_3H_4)I] and [Co(η^5-C_5H_5)(η^3-2-MeC_3H_4)(ACN)]BF_4, respectively, were used. The latter values were obtained using solutions of two authentic complexes of known concentration. In the case of [Co(η^5-C_5H_5)(η^3-2-MeC_3H_4)I], the spectrum was taken as soon as possible after the dissolution of the complex in order to minimize the variation in the absorbance due to reaction 8. From the linear plot representing $\ln[(A/c - \epsilon_P)/(\epsilon_R - \epsilon_P)]$ vs time at the two wavelengths considered, the value $k_8 = (6.5 \pm 0.8) \times 10^{-4}$ s^{-1} was obtained, in rather good agreement with that obtained from the conductivity measurements.

By performing digital simulations of the CV curves, knowledge of the rate constant k_8 allowed for evaluation of the time evolution of peak P_{C1}. In particular, the overall cathodic current i has been calculated as the sum of the current i_1 due to the reduction of [Co(η^5-C_5H_5)(η^3-2-MeC_3H_4)I] according to eqs 3 and 6 and of the current i_2 due to the reduction of [Co(η^5-C_5H_5)(η^3-2-MeC_3H_4)(ACN)]$^+$ formed according to eq 8. By considering that, in our conditions, the currents i_1 and i_2 are linear functions of the concentrations of [Co(η^5-C_5H_5)(η^3-2-MeC_3H_4)I] and [Co(η^5-C_5H_5)(η^3-2-MeC_3H_4)(ACN)]$^+$, respectively, the current i at any potential E is given by eq 9,

$$i = i_1 + i_2 = i_1^{\circ}(\exp(-k_8 t) + i_2^{\infty}(1-\exp(-k_8 t)) \quad (9)$$

where i_1° and i_2^{∞} are the experimental values of peak P_{C1} current at a given potential and at $t \approx 0$ and $t \geq 45$ min, respectively. The cathodic voltammetric curves calculated at times t = 10, 30, and 45 min according to eq 9 satisfactorily reproduce the corresponding experimental curves, confirming that the time evolution of peak P_{C1} is due to the occurrence of reaction 8.

Conclusions

The electrochemical reduction of [Co(η^5-C_5H_5)(η^3-2-MeC_3H_4)I] in ACN gives rise, in cyclic voltammetry, to two cathodic peaks, the first of which is irreversible both chemically and electrochemically while the second is reversible. The process corresponding to the first peak can be described in terms of a dissociative electron transfer in which the introduction of one electron induces metal−halide bond breaking, concerted with the electron transfer, with the formation of a neutral radical which, by fast solvation, gives rise to the solvato complex [Co(η^5-C_5H_5)(η^3-2-MeC_3H_4)(ACN)]$^{\bullet}$. Such a solvato complex then acts as an efficient electron donor toward the starting material, with the formation of [Co(η^5-C_5H_5)(η^3-2-MeC_3H_4)(ACN)]$^+$; finally, the cation is electroreduced at the working potentials to conclude an overall autocatalytic sequence. The solvato complex [Co(η^5-

$C_5H_5)(\eta^3\text{-}2\text{-}MeC_3H_4)(ACN)]^{\bullet}$, formed as a product of the above reduction process, can be reversibly reduced to the corresponding anion at more negative potentials. Confirmation of the above mechanism has been obtained by the study of the electrochemical behavior of the solvato complex $[Co(\eta^5\text{-}C_5H_5)(\eta^3\text{-}2\text{-}MeC_3H_4)(ACN)]^+$, kinetic analysis, and simulation of the experimental pattern.

The above behavior refers to CV experiments carried out within the first 5 min of dissolution of the complex. At longer times, the concomitant homogeneous solvolysis of the starting complex with the formation of the solvato complex $[Co(\eta^5\text{-}C_5H_5)(\eta^3\text{-}2\text{-}MeC_3H_4)(ACN)]^+$ has been considered in order to explain the time evolution of the CV curves. The occurrence of the bulk reaction between the starting complex and solvent has been confirmed by conductivity and spectroscopic measurements. In particular, from this type of measurements, the rate constant for the homogeneous solvolysis has been determined, thus allowing a satisfactory quantitative description of the time dependence of the CV curves.

Experimental Section

Instrumentation and Procedures. Voltammograms were recorded with an AMEL model 552 potentiostat controlled by an AMEL model 568 function generator, an AMEL model 865 A/D converter, a Hewlett-Packard 7475A digital plotter and a Nicolet model 3091 digital oscilloscope. The minimization of the uncompensated resistance effect in the voltammetric measurements was achieved by the positive-feedback circuit of the potentiostat. UV−Vis spectra were taken using a Varian Cary 5E UV−Vis−NIR spectrophotometer. Conductivity measurements were carried out with an AMEL model 133 conductivity meter. Temperature control was accomplished within 0.1 °C by a Lauda Klein-Kryomat thermostat.

The one-compartment electrochemical cell was of airtight design with high-vacuum glass stopcocks fitted with either Teflon or Kalrez (DuPont) O-rings in order to prevent contamination by grease. The connections to the high-vacuum line and to the Schlenk flask containing the solvent were obtained by spherical joints also fitted with Kalrez O-rings. The pressure measured in the electrochemical cell prior to performing the trap-to-trap distillation of the solvent was typically $2.0-3.0 \times 10^{-5}$ mbar. The working electrode consisted of a 0.6 mm in diameter platinum wire (0.15 cm^2 approximately) sealed in glass. The counter electrode consisted of a platinum spiral, and the quasi-reference electrode was a silver spiral. The quasi-reference electrode drift was negligible for the time required by a single experiment. Both the counter and reference electrodes were separated from the working electrode by ~0.5 cm. Potentials were measured with the ferrocene standard and are always referred to SCE. $E_{1/2}$ values correspond to $(E_{pc} + E_{pa})/2$. Ferrocinium/ferrocene couple standard potential measured with respect to SCE was +0.39 V at 25 °C. In some experiment SCE reference electrode was used, separated from the working electrode compartment by a sintered glass frit. Ferrocene was also used as internal standard for measuring the number of electrons corresponding to voltammetric peaks and to check the electrochemical reversibility of a redox couple. The DigiSim 2.1 software by Bioanalytical Systems Inc. was used to simulate all of the experimental curves.

Materials. The complexes $[Co(\eta^5\text{-}C_3H_5)(\eta^3\text{-}2\text{-}MeC_3H_4)I]$ and $[Co(\eta^5\text{-}C_5H_5)(\eta^3\text{-}2\text{-}MeC_3H_4)(ACN)]^+$ were obtained and purified following the literature procedures.[3f,19]

All materials were reagent grade chemicals. Tetraethylammonium tetrafluoroborate ($TEABF_4$, puriss. Fluka) and tetraethylammonium iodide (TEAI, puriss. Fluka) were used as received without any further purification.

Acetonitrile (ACN, UVASOL, Merck) was purified by refluxing over CaH_2 for several days under argon and successively distilling into a Schlenk flask containing thermally activated 4 Å molecular sieves. The solvent was then distilled, just prior to use, into the electrochemical cell using a trap-to-trap procedure.

Acknowledgment. This work was supported by the Ministero dell'Università e della Ricerca Scientifica e Tecnologica, by the Consiglio Nazionale delle Ricerche, and by the University of Bologna (Funds for Selected Research Topics).

OM9706368